Space resolved temperature measurements in an argon methane microwave plasma used for hydrogen production

S. Kreuznacht[1] , M. Böke[1] and A. von Keudell[1]

[1] *Chair for Experimental Physics II, Ruhr University Bochum, Bochum, Germany*

Abstract: The pyrolysis of methane is a promising, new, greenhouse gas-free production method of hydrogen. Here, we will present space resolved optical emission spectra of a microwave plasma torch operated in an argon methane mixture (up to 34 $\%_{vol}$ admixture). The emission spectra are dominated by dicarbon Swan bands and black body radiation. Both spectral features were utilized to estimate the gas temperature. In the center of the plasma gas temperatures of up to 4500 K are reached with large gradients (500 K/mm) in radial direction.

Keywords: methane pyrolysis, hydrogen production, microwave plasma, Swan bands

1. Introduction

Hydrogen is often regarded as green fuel of the future. Today, hydrogen is mainly produced by steam reforming of methane. Since this process emits a lot of CO_2 (11 tons of CO_2 per ton of H_2) [1], the production of hydrogen is already today responsible for 1 % to 2 % of the annual global greenhouse gas emission [2,3]. Therefore, new energy efficient and greenhouse gas-free production methods are in high demand. One promising production method is the pyrolysis of methane. In this process methane is thermally dissociated into hydrogen and solid carbon generating no direct greenhouse gas emissions. Instead, high purity solid carbon is produced as a second valuable product. The theoretical energy demand for the production of hydrogen by pyrolysis of methane (ΔH_0=0.39 eV/H_2 [4]) is about eight times lower compared to the production of hydrogen by electrolysis of water (ΔH_0=2.96 eV/H_2 [4]).

The main expected products for the pyrolysis of methane are hydrogen, acetylene, ethylene and solid carbon corresponding to the following global reactions:

$$2\ CH_4 \rightarrow 4\ H_2 + 2\ C_{(s)} \quad (1)$$

$$2\ CH_4 \rightarrow 3\ H_2 + C_2H_2 \quad (2)$$

$$2\ CH_4 \rightarrow 2\ H_2 + C_2H_4 \quad (3)$$

The highest possible hydrogen yield can be achieved by reaction (1). However, acetylene and ethylene are energetically more favorable secondary products due to their higher standard enthalpies of formation of 2.36 eV and 0.54 eV, respectively [4].

High energy inputs are necessary to dissociate methane due to the high average binding energy of the C-H bonds (4.31 eV [5]) in a methane molecule. A plasma can be used to supply the required activation energy either by high gas temperatures (above 1300 K [6]) or by electron impact dissociation. In the past, plasma sources operating at a pressure of a few mbar up to atmospheric pressure were investigated for the pyrolysis of methane. A microwave plasma torch (MPT) is one example with high performance in terms of energy efficiency and mass yield [7]. In a MPT, microwaves are coupled into a microwave transparent discharge tube to ignite and sustain a plasma. The process gas is injected into the discharge tube in a swirl flow to stabilize the plasma in the center of the tube and shield the walls from the hot core of the plasma. With MPTs gas temperatures above 4000 K can be reached in the center of the plasma without damaging the walls of the discharge tube [8,9]. At these high gas temperatures the chemistry is dominated by neutral species reactions while the reactivity due to ionic species and electrons can be neglected [7,10,11].

The gas temperature determines the rates of all reactions between neutral species and is therefore a very important parameter. Space resolved measurements of the local gas temperature within the plasma can help to get new insights into the complex interaction between plasma physics, fluid dynamics and chemistry within the MPT and optimize the methane pyrolysis for maximum conversion, desired product spectrum and energy efficiency. Here, optical emission spectroscopy was used to determine the local gas temperature from the emission of the dicarbon Swan bands and the black body radiation from the surface of the hot carbon particles produced in the MPT.

2. Experiment

The used MPT is a commercially available plasma source from MUEGGE (type MA6000A-013BB). Microwaves with a frequency of 2.45 GHz and input powers of up to 6 kW are supplied via a waveguide including a 3-stub tuner and a circulator into a cylindrical resonator. The forward and reflected power are measured yielding the power absorbed by the plasma. A quartz tube (26 mm inner diameter, 740 mm length) is positioned on the central axis of the resonator. The plasma is ignited in this tube by injecting a tungsten tip for 200 ms into the quartz tube. Argon with admixtures of 1 $\%_{vol}$ to 34 $\%_{vol}$ of methane was used as process gas at atmospheric pressure. The process gas is supplied via eight tangential nozzles into the quartz tube to create a swirl flow. The flow rate was set to 60 slm. A more detailed description of the MPT can be found elsewhere [13].

A cyclone was connected downstream of the MPT to separate the carbon particles from the product gas stream. The product gas stream was split into two parts. 1 slm was analysed with a continuous gas analyser (Emerson xStream) with infrared channels for methane, acetylene

and ethylene and a thermal conductivity channel for hydrogen.

Figure 1 shows the optical emission spectrum of the plasma. The spectrum is dominated by a broadband continuum caused by the black body radiation emitted from the hot carbon particles and molecular emission bands of the dicarbon Swan band ($d^3\Pi_g$-$a^3\Pi_u$). Both features of the spectrum can be used to estimate the local gas temperature. Therefore, a broadband spectrograph (Ocean Optics USB4000) was used to measure the black body radiation and a high resolution spectrograph (Acton Research SpectraPro 750) was used to resolve the Swan bands. Both spectrographs were connected by a multicore fibre optic to a collimator. The collimator was mounted on a two axis stepping motor to move it perpendicular and in direction of the gas flow along the quartz tube.

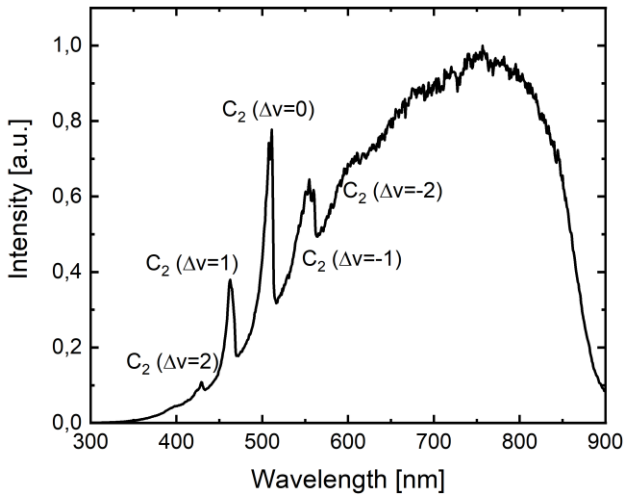

Fig. 1. Optical emission spectrum of the microwave plasma torch operated in argon with 4 $\%_{vol}$ methane admixture.

Additionally, a CMOS camera (Raspberry Pi Zero W with high quality camera module) was used to measure the radial extension of the plasma directly below the resonator.

3. Results and discussion

Figure 2 shows the conversion as a function of the methane admixture and the specific energy input (SEI). The specific energy input is the power absorbed by the plasma divided by the input amount of methane. The methane conversion increases linearly with the SEI at constant methane admixture. Increasing the methane admixture at constant SEI also leads to an increase in methane conversion and consequently to a higher energy efficiency.

Figure 3 shows the relative emission intensity of the plasma directly below the resonator as a function of the position perpendicular to the gas flow and the SEI at 2 $\%_{vol}$ methane admixture. The intensity profils have a minimum in the center of the plasma and two maxima on both sides from the center. The positions of these two maxima shift further to the outside when increasing the SEI indicating an increase of the radial extension of the plasma with increasing SEI. To further investigate this, the squared position of the two maxima is plotted as a function of the SEI in figure 4. Because of the cylindrical symmetry of the system, the squared position is proportional to the area of the plasma in a cut plane perpendicular to the gas flow. The squared position of both maxima increases linearly with the SEI explaining the increase in methane conversion with increasing SEI. When increasing the SEI the radial extension of the plasma increases leading to a larger portion of the gas passing through the plasma leading to a larger conversion.

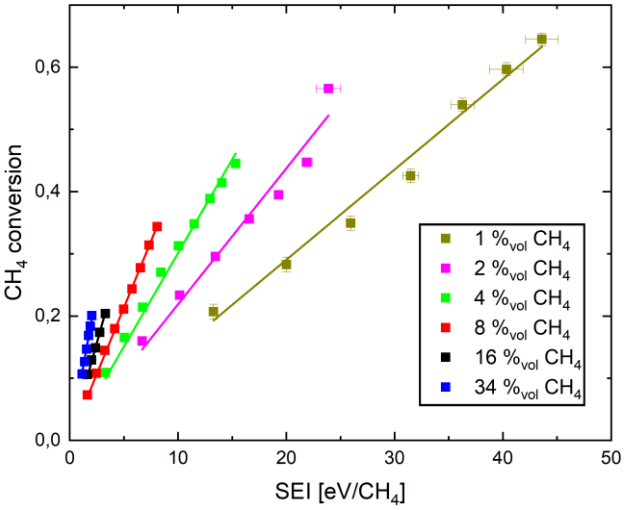

Fig. 2. Methane convsion as a function of the specific energy input (SEI) and methane admixture.

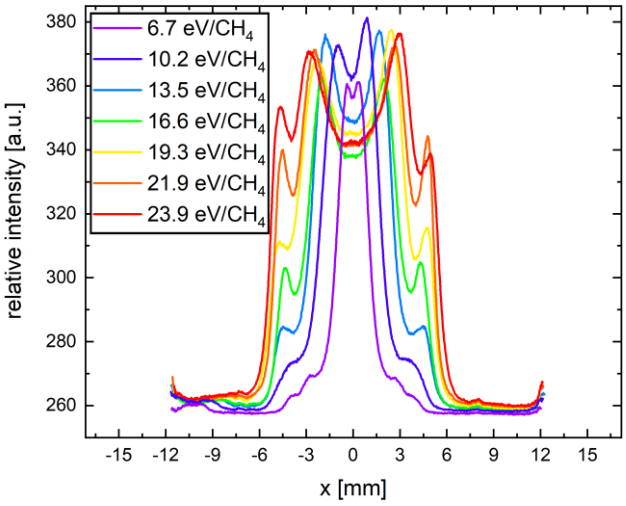

Fig. 3. Relative intensity as a function of the specific energy input (SEI) and position perpendicular to the gas flow measured with the CMOS camera at 2 $\%_{vol}$ CH_4 admixture.

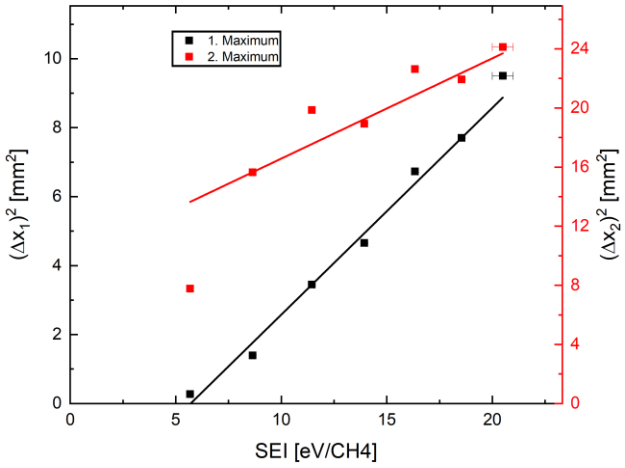

Fig. 4. Squared position of the two emission intensity maxima extracted from figure 3 as a function of the specific energy input.

To further investigate the spatial extension of the plasma, optical emission spectroscopy was used to resolve the emission of the dicarbon Swan bands and of the black body radiation in radial and axial direction. During operation the quartz tube is getting coated by a thin layer of carbon particles. In continuous operation a dynamic equilibrium establishes between deposition of new carbon particles on the wall and removal of particles by the strong gas flow from the wall. This prevents the carbon layer from growing thicker than about 1 mm. The carbon layer does not hinder the operation of the setup even after several days of operation without cleaning of the quartz tube. space resolve spectroscopy of the plasma emission is restricted by this carbon layer to the first 45 mm below the resonator. Further downstream the growth of the carbon layer is to fast and the emission from the plasma to dim for measuring any spectra.

The emission of the plasma was sampled with the collimator with a step size of 0.25 mm in radial direction and 5 mm in axial direction and subsequently analysed with the two spectrographs. The cylindrical symmetry of the system was used to calculate the emissivity of the plasma from the line of sight integrated measured intensities using Abel inversion. A deconvolution procedure with Tikhonov regularization was used to perform the Abel inversion [14,15]. The finite-difference matrix was used as Tikhonov matrix and the optimal Tikhonov parameter for each wavelength of the spectra was calculated using generalized cross validation [16]. The high resolution spectra of the Swan bands were subsequently fitted with a custom Matlab app based on the theory of emission spectra of diatomic molecules [17] and on the molecular constants for the dicarbon Swan bands [18] to obtain the rotational temperature. The spectra of the black body radiation were fitted using Planck's law to obtain the surface temperature of the hot carbon particles. Both temperatures can be used to estimate the local gas temperature.

Figure 5 shows the resulting gas temperature, emission intensity of the black body radiation and emission intensity of the dicarbon Swan bands as a function of the radial and axial position for three different sets of operating parameters. Both the black body radiation and the emission from the dicarbon Swan bands have one intensity maximum in radial direction. The radial position of these maxima is identical to the position of the outer and inner maxima observed in the camera images respectively. Due to the emission intensity profil of the black body radiation and of the dicarbon Swan bands, the rotational temperature of the dicarbon molecules was used to estimate the local gas temperature in the center of the plasma and the black body temperature was used to estimate the local gas temperature further outside. In the center of the plasma a gas temperature of up to 4600 K is reached. The temperature decreases in radial direction by about 500 K/mm and in axial direction by about 50 K/mm. The temperature profil together with the chemistry of methane explains the different spatial position of the emission maxima. The local gas temperature in the center of the plasma is to high to form solid carbon (sublimation temperature 3915 K). The emission intensity maximum of the black body radiation is located at a position where the local gas temperature is around 1900 K. This matches the temperature at which the rate for nucleation and growth of solid carbon particles is maximal [6]. Dicarbon, on the other hand, is only produced at temperatures between 4000 K and 5000 K [6]. Therefore, the dicarbon Swan bands are only emitted close to the center of the plasma. Changing the SEI or methane admixture has almost no effect on the maximum temperature in the center of the plasma. However, with increasing SEI the size of the high temperature region growth in axial and radial direction. This leads to a shift of the emission intensity maxima further outside caused by the broadening of the temperature profil. Increasing the methane admixture has the same effect. However, changing the SEI has a larger impact compared to changing the methane admixture.

Methane dissociation begins at 770 K and is completed at 1470 K in thermal equilibrium. At temperatures above 2000 K methane is converted on a timescale of less than 0.7 ms [6]. This is way below the residence time in these temperature regions (several 10 ms). Therefore, methane is fully converted in the high temperature region of the setup. The overall conversion is controlled by the fraction of input gas passing trough the high temperature region. The overall conversion can be increased by increasing the radial extension of the high temperature region.

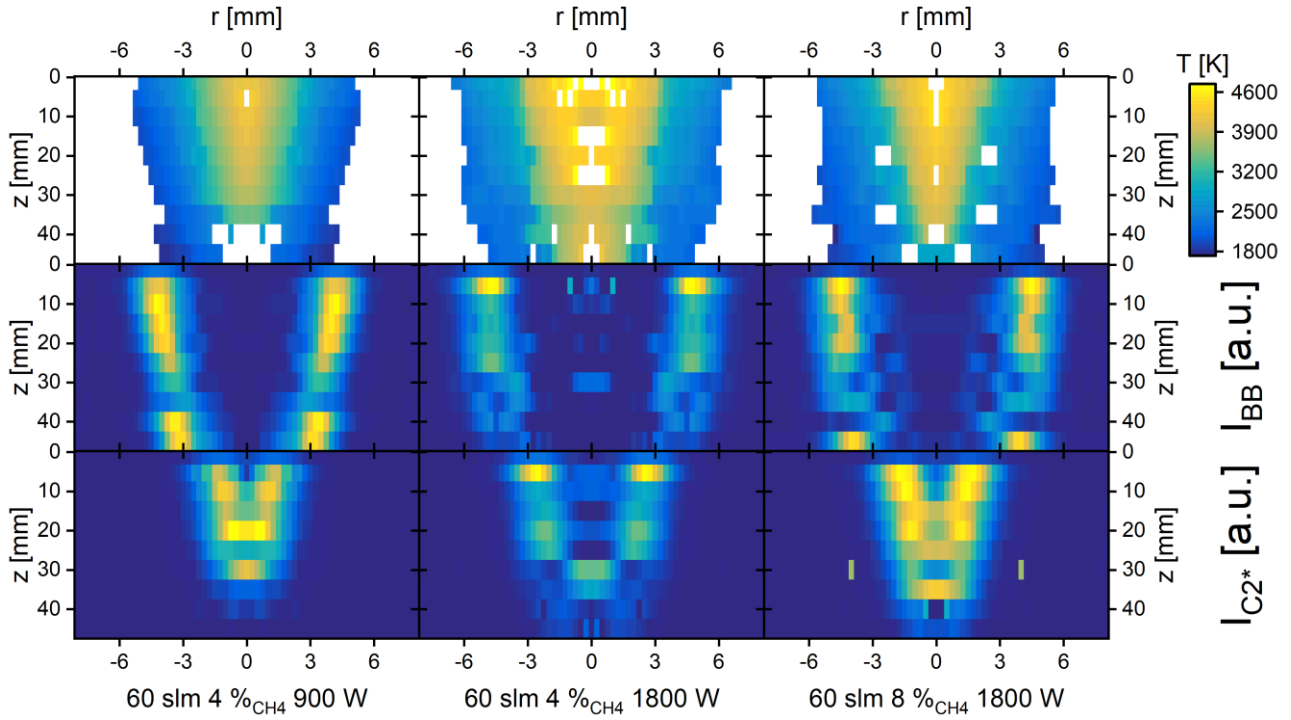

Fig. 5. Gas temperature, black body radiation emission intensity (I_{BB}) and dicarbon Swan bands emission intensity (I_{C2^*}) as function of the radial and axial position for three different sets of operating parameters.

4. Conclusion

Methane pyrolysis in an atmospheric pressure microwave plasma torch was investigated. The methane conversion increases linearly with the SEI. At constant SEI methane conversion increases with increasing methane admixture. In the center of the plasma gas temperatures of up to 4500 K are reached leading to a rapid conversion of methane. The gas temperature decreases in radial direction by about 500 K/mm. This limites the methane conversion to the central high temperature region of the setup and also leads to a narrow nucleation and growth region for the solid carbon particles.

5. Acknowledgment

This work was supported by the German Federal Ministry of Education and Research within 03SF0571C.

6. References

[1] O. Machhammer, Chemie Ingenieur Technik, 87: 409-418 (2015)
[2] International energy agency, The future of hydrogen (2019)
[3] J. Gütschow, A. Günther, M. Pflüger, Earth System. Sci. Data, 8, 571-603 (2016)
[4] D. R. Burgess Jr., NIST Chemistry Webbook, Thermochemical Data (2022)
[5] J. Huheey, E. Keiter, R. Keiter, De Gruyter, Anorganische Chemie, 322 (2014)
[6] J. R. Fincke, R. P. Anderson, T. A. Hyde, B. A. Detering, Industrial & Engineering Chemistry Research, 41, 1425–1435 (2002)
[7] M. Scapinello, E. Delikonstantis, G. D. Stefanidis, Chemical Engineering and Processing: Process Intensification, 117, 120-140 (2017)
[8] M. Leins, M. Walker, A. Schulz, U. Schumacher, U. Stroth, Contributions to Plasma Physics, 52, 615-628 (2012)
[9] M. Jasiński, D. Czylkowski, B. Hrycak, M. Dors, J. Mizeraczyk, International Journal of Hydrogen Energy, 38, 11473-11483 (2013)
[10] A. Magazova, S. Böddeker, N. Bibinov, D. W. Agar, Chemie Ingenieur Technik, 94, 690-700 (2022)
[11] T. Kovács, Plasma Chem Plasma Process, 30, 207–212 (2010)
[12] E. Carbone, F. D'Isa, A. Hecimovic, U. Fantz, Plasma Sources Science and Technology, 29.5 (2020)
[13] M. Leins, J. Kopecki, S. Gaiser, A. Schulz, M. Walker, U. Schumacher, U. Stroth, T. Hirth, Contributions to Plasma Physics, 54,14-26 (2014)
[14] K. J. Daun, K. A. Thomson, F. Liu, G. J. Smallwood, Appl. Opt. 45, 4638-4646 (2006)
[15] D. D. Hickstein, S. T. Gibson, R. Yurchak, D. D. Das, M. Ryazanov Review of Scientific Instruments, 90, 065115 (2019)
[16] F. Bauer, M. A. Lukas, Mathematics and Computers in Simulation, 81, 1795-1841 (2011)
[17] I. Kovacs, Budapest: Akadémiai Kiadó (1969)
[18] J. S. A. Brooke, P. F. Bernath, T. W. Schmidt, G. B. Bacskay, Journal of Quantitative Spectroscopy and Radiative Transfer, 124, 11-20 (2013)